OL Organic Letters

pubs.acs.org/OrgLett Letter

A Proline-Squaraine Ligand Framework (Pro-SqEB) for Stereoselective Rhodium(II)-Catalyzed Cyclopropanations

Emily P. Bacher,[†] Raïssa Twiringiyimana,[†] Kevin X. Rodriguez, Renita A. Wilson, Alexandra K. Bodnar, Ryan O'Connell, Tiffany A. Toni, Kaitlyn E. Eckert, Olaf Wiest,* and Brandon L. Ashfeld*

Cite This: *Org. Lett.* 2023, 25, 8156–8161 Read Online

ACCESS | Metrics & More | Article Recommendations | Supporting Information

ABSTRACT: A proline-squaraine ligand (Pro-SqEB) that demonstrates high levels of stereoselectivity in olefin cyclopropanations when anchored to a Rh_2^{II} scaffold is introduced. High yields and enantioselectivities were achieved in the cyclopropanation of alkenes with diazo compounds in the presence of Rh_2(Pro-SqEB)$_4$. Notably, the unique electronic and steric design of this catalyst enabled the use of polar solvents that are otherwise incompatible with most Rh^{II} complexes.

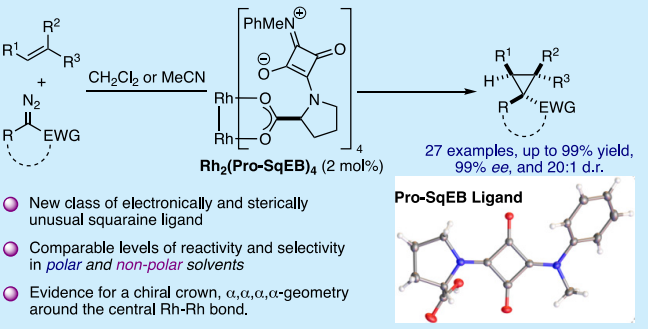

The development of enantioselective, transition-metal-catalyzed transformations inevitably coincides with the search for new classes of chiral ligand scaffolds. Stability, modular flexibility, and readily accessible sources of chirality are among a host of important factors in scaffold design. Emergence of the 1,2-squaramide motif in Brønsted acid catalysis has led to an assortment of enantioselective C−C bond constructions.[1] Interestingly, the central cyclobutenedione core is often overlooked as a point of modification, and the exploitation of this scaffold in transition metal catalysis is significantly underdeveloped.[2] In contrast, 1,3-squaraines represent a fascinating bonding motif of relatively unexplored synthetic potential.[3] Perhaps best known for their chromophoric properties and use in noninvasive imaging of biological processes, physical and analytical chemistry,[4] squaraines are characterized by a highly electrophilic cyclobutenone core that frequently presents a hindrance to their broader applicability.[5] However, we envisioned that the rigidity and donor−acceptor charge distribution would present an intriguing opportunity in catalysis, wherein the cyclobutenedione core serves as a central motif in order to impart the requisite electronic and structural features necessary for high levels of stereoinduction.

To the best of our knowledge, the 1,3-squaramide-catalyzed Reformatsky reaction reported by Heng et al. in 2002 constitutes the only reported example of a chiral 1,3-squaramide ligand−metal complex in enantioselective C−C bond construction (Figure 1a).[6] We speculated that a proline-derived 1,3-squaramide would provide a versatile carboxylate ligand template in transition metal catalysis. The rich history of chiral Rh^{II} carboxylates in enantioselective catalysis, characterized by a high degree of organized symmetry arising from the paddlewheel orientation around the central Rh−Rh bond,

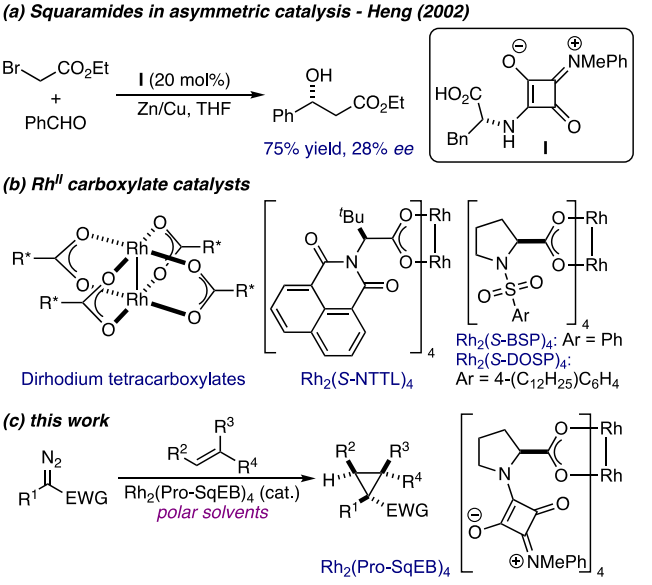

Figure 1. Chiral Rh^{II} complexes in catalysis.

serves as a basis for evaluating new ligand scaffolds (Figure 1b).[7] Pioneered by the seminal contributions of Davies and

Received: October 16, 2023
Revised: October 30, 2023
Accepted: October 30, 2023
Published: November 8, 2023

Doyle, the predictable ligation properties of carboxylates and carboxamides has inspired the design and implementation of new ligands in enantioselective Rh^{II}-catalyzed transformations.[8] Herein, we report the first use of an aminoacid-derived 1,3-squaramide as a core template for the design of new ligands in Rh^{II} catalysis by showcasing the enantioselective cyclopropanation of alkenes with diazo compounds in the presence of Rh_2(Pro-SqEB)$_4$ (Figure 1c).

Preparation of the chiral 1,3-squaramide began with the addition of L-proline to isosquaramide **1**[6] to give Pro-SqEB (**2**) in quantitative yield, and 90% over two steps from squaric acid (Scheme 1). The relative 1,3-configuration was confirmed

Scheme 1. Synthesis of Rh_2(Pro-SqEB)$_4$

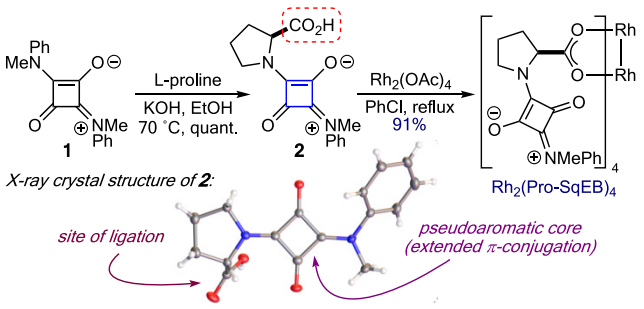

by X-ray crystallography and revealed an *anti*-orientation of the amide *N*-phenyl substituent and proline carboxylic acid across the central ring. Transligation of $Rh_2(OAc)_4$ provided Rh_2(Pro-SqEB)$_4$ in 91% yield.

We next sought to benchmark the efficiency and stereoselectivity of Rh_2(Pro-SqEB)$_4$ in the cyclopropanation of alkenes. Thus, addition of diazo ester **3a** over 1 h to styrene (**4a**) and Rh_2(Pro-SqEB)$_4$ in CH_2Cl_2 at 40 °C led to an 84% yield of **5a** in 54% *ee* as a single diastereomer (Table 1, entry 1). Encouraged by this initial result, we began the reaction optimization by lowering the temperature to −20 °C, which improved the enantioselectivity to 78% *ee* (entry 2). While conducting the reaction in MeCN at 40 °C led to comparable results, performing the reaction at −20 °C improved selectivity (entries 3 and 4). Decreasing the reaction concentration and

Table 1. Cyclopropanation Optimization between Methyl Phenyldiazoacetate (3a) and Styrene (4a)[a]

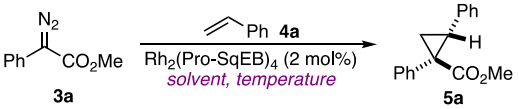

entry	solvent	temp (°C)	yield (%)	*ee* (%)
1	CH_2Cl_2	40	84	54
2	CH_2Cl_2	−20	77	78
3	MeCN	40	66	78
4	MeCN	−20	67	90
5[b]	MeCN	−20	>99	90
6[c]	***MeCN***	***−20***	***>99***	**99**
7	MeCN/$MeNO_2$ (2:1)	0	>99	88
8	hexanes	rt	<5	8

[a]Conditions: Slow addition over 1 h of **3a** (0.15 mmol) to **4a** (0.45 mmol) and Rh_2(Pro-SqEB)$_4$ (1 mol %) at 0.1 M. [b]Reaction concentration = 0.0167 M. [c]Relative stoichiometry: **3a** (0.1 mmol) to **4a** (0.05 mmol).

surveying the medium polarity minimized **3a** dimerization leading to **5a** in an optimized >99% yield and 99% *ee* (entries 5−7). Nonpolar solvents (i.e., hexanes) led to a dramatic decrease in both yield and enantioselectivity (entry 8). This is notable given the high enantio- and diastereoselectivities observed with Rh_2(*S*-TBSP)$_4$ and Rh_2(*S*-DOSP)$_4$ in nonpolar, hydrocarbon solvents.[9] This observation is significant in that an increased solvent polarity range improves the applicability of this powerful transformation to biologically relevant systems.

To evaluate the efficiency and stereoselectivity of the cyclopropanation, we compared and contrasted Rh_2(Pro-SqEB)$_4$, Rh_2(*S*-DOSP)$_4$, and Rh_2(*S*-NTTL)$_4$, the latter chosen for the high levels of enantioselectivity observed across an array of diazo compounds that includes diazo oxindoles (Table 2).[10] For comparison, we employed reaction conditions previously shown optimal in Rh^{II}-catalyzed cyclopropanations (CH_2Cl_2, 0 °C to rt).[10b,11] In general, Rh_2(Pro-SqEB)$_4$ provided the corresponding cyclopropanes in improved or comparable stereoselectivity with **3a**. For example, the cyclopropanation of styrene and its derivatives **4a−c** yielded adducts **5a−c** in 63−99% yield and 68−92% *ee* with Rh_2(Pro-SqEB)$_4$. However, the Rh_2(Pro-SqEB)$_4$-catalyzed cyclopropanation of **4d** provided **5d** in 77% yield, 43% *ee*, and >20:1 dr, while Rh_2(*S*-DOSP)$_4$ proceeded in 78% yield, 72% *ee*, and >20:1 dr. Additionally, performing the reaction in MeCN at −20 °C afforded the cyclopropanes in improved yield and selectivity. For example, the Rh_2(Pro-SqEB)$_4$-catalyzed cyclopropanation of **4e** under our optimized conditions afforded **5e** in 99% yield and 96% *ee*, while Rh_2(*S*-DOSP)$_4$ led to only recovered starting material. Under our optimized conditions, Rh_2(*S*-DOSP)$_4$ afforded **5d** in higher enantioselectivity (72% *ee*) compared to Rh_2(Pro-SqEB)$_4$ (58% *ee*). Although Rh_2(Pro-SqEB)$_4$ provided **5f** in a 3:1 dr (Rh_2(*S*-NTTL)$_4$: dr >20:1), the enantioselectivities were significantly higher and the yields were comparable between Rh_2(Pro-SqEB)$_4$ and Rh_2(*S*-DOSP)$_4$. In contrast, **4g** gave comparably low yields and diastereoselectivities with both catalysts, but Rh_2(*S*-NTTL)$_4$ provided **5g** with significantly higher enantioselectivity. Conducting the cyclopropanation with Rh_2(Pro-SqEB)$_4$ in MeCN at −20 °C provided **5g** in 99% yield and 80% *ee*, while Rh_2(S-DOSP)$_4$ did not lead to the formation of the product. Notably, X-ray crystallographic analysis of **5a** confirmed that Rh_2(*S*-NTTL)$_4$ proceeded with an opposite sense of enantioinduction to the other catalysts.

Diazo oxindoles represent an intriguing architectural framework, the reactivity of which often differs from that of other donor−acceptor diazo compounds. The resulting spirooxindoles can serve as building blocks in the construction of biologically active alkaloids, and highly enantioselective cyclopropanations involving diazo oxindoles are rare.[12] We sought to evaluate the efficacy of Rh_2(Pro-SqEB)$_4$ in cyclopropanations with *N*-methyl diazo oxindole (**6a**) (Table 3). In general, Rh_2(*S*-NTTL)$_4$ provided the desired cyclopropanes with higher levels of enantio- and diastereoselectivity than those of Rh_2(Pro-SqEB)$_4$ and Rh_2(*S*-DOSP)$_4$. However, the Rh_2(Pro-SqEB)$_4$-catalyzed cyclopropanation of **4g** provided **7g** in 89% yield, 55% *ee*, and >20:1 dr, while Rh_2(*S*-NTTL)$_4$ proceeded in 67% yield, 7% *ee*, and >20:1 dr. In addition, performing the reaction in MeCN at −20 °C with Rh_2(Pro-SqEB)$_4$ afforded **7a** in 99% yield, 96% *ee*, >20:1 dr; **7f** in 86% yield, 54% *ee*, >20:1 dr; and **7h** in 99% yield, 64% ee, >20:1 dr. In contrast, similar reactions with Rh_2(*S*-DOSP)$_4$ in

https://doi.org/10.1021/acs.orglett.3c03344
Org. Lett. 2023, 25, 8156−8161

Table 2. Comparative Cyclopropanations with Methyl Phenyldiazoacetate (3a)[a]

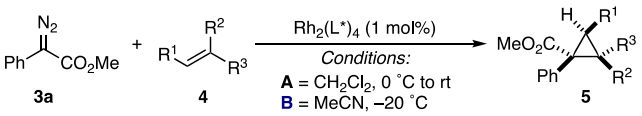

3a 4 5

Product	A/B	Pro-SqEB	*S*-DOSP	*S*-NTTL
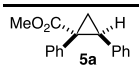 5a	A	99% yield	94% yield	72% yield
		92% *ee*	68% *ee*	32% *ee*
		dr >20:1	dr >20:1	dr >20:1
	B	99% yield	28% yield	–
		99% *ee*	66% *ee*	
		dr >20:1	dr >20:1	
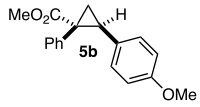 5b	A	63% yield	78% yield	51% yield
		81% *ee*	80% *ee*	41% *ee*
		dr >20:1	dr >20:1	dr = 17:1
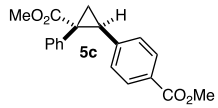 5c	A	73% yield	70% yield	63% yield
		82% *ee*	68% *ee*	34% *ee*
		dr >20:1	dr >20:1	dr >20:1
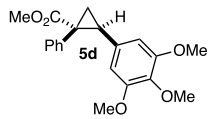 5d	A	77% yield	78% yield	77% yield
		43% *ee*	72% *ee*	5% *ee*
		dr >20:1	dr >20:1	dr >20:1
	B	99% yield	36% yield	–
		58% *ee*	72% *ee*	
		dr >20:1	dr >20:1	
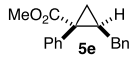 5e	A	49% yield	34% yield	54% yield
		61% *ee*	32% *ee*	20% *ee*
		dr >20:1	dr >20:1	dr >20:1
	B	99% yield	0% yield	–
		96% *ee*		
		dr >20:1		
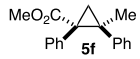 5f	A	63% yield	70% yield	52% yield
		71% *ee*	48% *ee*	39% *ee*
		dr = 3:1	dr = 2:1	dr >20:1
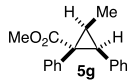 5g	A	39% yield	74% yield	36% yield
		7% *ee*	34% *ee*	69% *ee*
		dr = 4:1	dr = 2:1	dr = 4:1
	B	99% yield	0% yield	–
		80% *ee*		
		dr = 4:1		
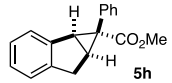 5h	A	99% yield	81% yield	70% yield
		73% *ee*	68% *ee*	19% *ee*
		dr = 10:1	dr = 4:1	dr = 8:1

[a]Major enantiomer shown employing Rh_2(Pro-SqEB)$_4$.

MeCN at −20 °C did not lead to the formation of the desired product.[13]

Table 3. Comparative Cyclopropanations with *N*-Methyl Diazooxindole (6a)[a]

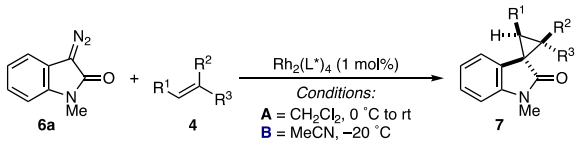

6a 4 7

Product	A/B	Pro-SqEB	*S*-DOSP	*S*-NTTL
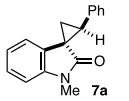 7a	A	99% yield	47% yield	97% yield
		51% *ee*	10% *ee*	93% *ee*
		dr >20:1	dr = 1:1	dr = 12:1
	B	99% yield	0% yield	–
		96% *ee*		
		dr >20:1		
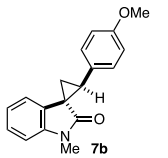 7b	A	80% yield	–	99% yield
		49% *ee*		89% *ee*
		dr = 6:1		dr = >20:1
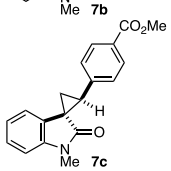 7c	A	74% yield	–	99% yield
		56% *ee*		82% *ee*
		dr >20:1		dr = 5:1
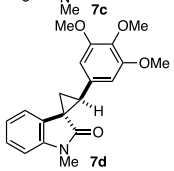 7d	A	74% yield	–	94% yield
		46% *ee*		84% *ee*
		dr = 7:1		dr >20:1
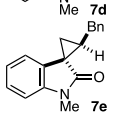 7e	A	31% yield	–	99% yield
		40% *ee*		93% *ee*
		dr = 6:1		dr = 5:1
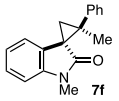 7f	A	84% yield	59% yield	59% yield
		95% *ee*	6% *ee*	93% *ee*
		dr >20:1	dr = 2:1	dr >20:1
	B	86% yield	0% yield	–
		54% *ee*		
		dr >20:1		
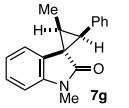 7g	A	89% yield	–	67% yield
		55% *ee*		7% *ee*
		dr >20:1		dr >20:1
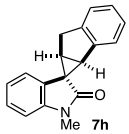 7h	A	92% yield	69% yield	69% yield
		71% *ee*	0% *ee*	0% *ee*
		dr >20:1	dr >20:1	dr >20:1
	B	99% yield	0% yield	–
		64% *ee*		
		dr >20:1		

[a]Major enantiomer shown employing Rh_2(Pro-SqEB)$_4$.

To date, a suitable crystal of Rh_2(Pro-SqEB)$_4$ for X-ray diffraction has remained elusive. We sought to gain insight into the geometrical configuration of the prolinate-squaraine ligands around the central Rh−Rh bond using computational

https://doi.org/10.1021/acs.orglett.3c03344
Org. Lett. 2023, 25, 8156−8161

methods. Overall, there are four possible orientations about the central Rh−Rh bond that the complex can adopt, namely, $\alpha,\alpha,\alpha,\alpha$ (C_4 symmetrical catalyst), $\alpha,\alpha,\alpha,\beta$ (C_1 asymmetrical catalyst), $\alpha,\alpha,\beta,\beta$ (C_2 symmetrical catalyst), or $\alpha,\beta,\alpha,\beta$ (D_2 symmetrical catalyst). It was shown that by considering the conformation of the catalyst, simple stereoselectivity models can be derived that are in good agreement with experimental observations and explicit computational studies of the relevant transition states.[10b,14] Using multilinear regression, analysis of the catalyst structure allowed for quantitative predictions of catalyst performance. However, the reactive conformation of the catalyst and those factors which determine the conformational equilibria are unclear. For example, Hashimoto reported the crystal structure of the phthalimido Rh_2(*S*-PTPA)$_4$ catalyst to be C_2-symmetric,[15] while the closely related crystal structure of naphthylmido Rh_2(*S*-NTTL)$_4$ is C_4 symmetric,[14] possibly due to π-stacking of the naphthyl moieties between adjacent molecules in the crystal.

For Rh_2(Pro-SqEB)$_4$, the question of conformational equilibria is complicated by the zwitterionic nature of the squaraine core, which could outweigh the π-stacking and hydrophobic effects that stabilize the C_4 conformation. To investigate the relative energies of the four conformers (C_4, C_1, C_2, D_2), DFT studies of the Rh_2(Pro-SqEB)$_4$ and the reference Rh_2(*S*-NTTL)$_4$ catalyst were performed using G16[16] at the B3LYP+D3/6-31+G*//6311+G**,LanL2DZ + PCM (acetonitrile) level of theory (Table 4). It should be noted that all calculations were performed without symmetry constraints, resulting in structures of approximate symmetry. For consistency with earlier studies, this nomenclature continues to be used here.

Table 4. Relative Energies (kcal/mol) of the Conformations of Rh_2(*S*-NTTL) and Rh_2(Pro-SqEB)$_4$

Conformation Symmetry	Rh_2(Pro-SqEB)$_4$	Rh_2(*S*-NTTL)$_4$
$\alpha,\alpha,\alpha,\alpha$ (C_4)	0	0
$\alpha,\alpha,\alpha,\beta$ (C_1)	7.2	6.7
$\alpha,\alpha,\beta,\beta$ (C_2)	17.3	7.0
$\alpha,\beta,\alpha,\beta$ (D_2)	7.9	15.5

The predicted C_4 conformation is significantly more stable for Rh_2(Pro-SqEB)$_4$ than the C_1, C_2, and D_2 conformations. These results are in good agreement with previous studies,[17] and the crystal structure of Rh_2(*S*-NTTL)$_4$,[14] thus validating the computational approach. Likewise, the predicted C_4 conformation for Rh_2(Pro-SqEB)$_4$ is substantially more stable, making the other conformations unlikely. Analysis of the C_4 structure, shown in Figure 2 (left), suggests that the 1,3-squaramide motifs, especially the negatively charged carbonyl groups, are positioned too far from the polar regions to result in significant electrostatic repulsion. Instead, edge-to-face stacking of the aromatic groups dominates, leading to a crown-like chiral environment similar to other chiral dirhodium catalysts.

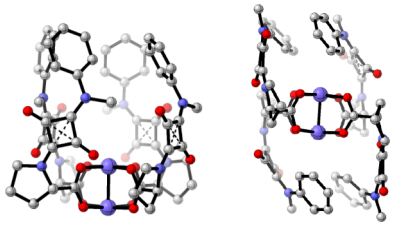

Figure 2. Calculated structures of C_4 (left) and D_2 (right) Rh_2(Pro-SqEB)$_4$ conformers. Hydrogens are hidden for clarity.

In comparison to Rh_2(*S*-NTTL)$_4$, the C_1 conformer of Rh_2(Pro-SqEB)$_4$ is calculated to be 7.2 kcal/mol higher in energy than C_4. The D_2 configuration is calculated to be 7.9 kcal/mol higher in energy, which marks a deviation from the relative trend of the NTTL ligand system. This is due to the favorable slipped $\pi-\pi$ stacking of the phenyl rings shown in Figure 2 (right), which is not possible in the more rigid Rh_2(*S*-NTTL)$_4$ framework. The C_2 conformer at 17.3 kcal/mol is the highest in energy, with the differences to the lowest energy C_4 structure being even larger than the high-energy conformations of Rh_2(S-NTTL)$_4$.

In conclusion, this work introduces chiral 1,3-squaramides as a new class of Rh-carboxylate ligands in enantioselective metallocarbene catalysis. The synthetic accessibility and ability to diversify the squaraine scaffold provide ample opportunities for future catalyst and reaction designs. The 1,3-squaramide ligand enables the execution of enantioselective cyclopropanations under polar reaction conditions, an environment that is often incompatible with many chiral Rh^{II} catalysts. Current efforts investigating the coordination chemistry of this ligand scaffold and its use in enantioselective transformations are ongoing and will be reported in due course.

■ ASSOCIATED CONTENT

Data Availability Statement

The data underlying this study are available in the published article and its Supporting Information.

Supporting Information

The Supporting Information is available free of charge at https://pubs.acs.org/doi/10.1021/acs.orglett.3c03344.

Experimental procedures, spectroscopic data, crystallographic data for **2**, and details of the computational studies, including Cartesian coordinates and energies of all species discussed (PDF)

Accession Codes

CCDC 2215242 contains the supplementary crystallographic data for this paper. These data can be obtained free of charge via www.ccdc.cam.ac.uk/data_request/cif, or by emailing data_request@ccdc.cam.ac.uk, or by contacting The Cambridge Crystallographic Data Centre, 12 Union Road, Cambridge CB2 1EZ, UK; fax: +44 1223 336033.

■ AUTHOR INFORMATION

Corresponding Authors

Brandon L. Ashfeld − *Department of Chemistry and Biochemistry, University of Notre Dame, Notre Dame, Indiana 46556, United States;* orcid.org/0000-0002-4552-2705; Email: bashfeld@nd.edu

Olaf Wiest − *Department of Chemistry and Biochemistry, University of Notre Dame, Notre Dame, Indiana 46556, United States;* orcid.org/0000-0001-9316-7720; Email: owiest@nd.edu

Authors

Emily P. Bacher − *Department of Chemistry and Biochemistry, University of Notre Dame, Notre Dame, Indiana 46556, United States*

https://doi.org/10.1021/acs.orglett.3c03344
Org. Lett. 2023, 25, 8156−8161

Raïssa Twiringiyimana − *Department of Chemistry and Biochemistry, University of Notre Dame, Notre Dame, Indiana 46556, United States*
Kevin X. Rodriguez − *Department of Chemistry and Biochemistry, University of Notre Dame, Notre Dame, Indiana 46556, United States*
Renita A. Wilson − *Department of Chemistry and Biochemistry, University of Notre Dame, Notre Dame, Indiana 46556, United States*
Alexandra K. Bodnar − *Department of Chemistry and Biochemistry, University of Notre Dame, Notre Dame, Indiana 46556, United States*
Ryan O'Connell − *Department of Chemistry and Biochemistry, University of Notre Dame, Notre Dame, Indiana 46556, United States*
Tiffany A. Toni − *Department of Chemistry and Biochemistry, University of Notre Dame, Notre Dame, Indiana 46556, United States*
Kaitlyn E. Eckert − *Department of Chemistry and Biochemistry, University of Notre Dame, Notre Dame, Indiana 46556, United States*

Complete contact information is available at: https://pubs.acs.org/10.1021/acs.orglett.3c03344

Author Contributions

†E.P.B. and R.T. contributed equally.

Notes

The authors declare no competing financial interest.

■ ACKNOWLEDGMENTS

The work in this manuscript was supported by the National Science Foundation (CHE-1956170 to B.L.A. and CHE-2247232 to O.W.). We would like to thank Dr. Allen Oliver (Department of Chemistry and Biochemistry, University of Notre Dame) for X-ray crystallography assistance.

■ REFERENCES

(1) (a) Chauhan, P.; Mahajan, S.; Kaya, U.; Hack, D.; Enders, D. Bifunctional Amine-Squaramides: Powerful Hydrogen-Bonding Organocatalysts for Asymmetric Domino/Cascade Reactions. *Adv. Synth. Catal.* **2015**, *357* (2−3), 253−281. (b) Malerich, J. P.; Hagihara, K.; Rawal, V. H. Chiral Squaramide Derivatives are Excellent Hydrogen Bond Donor Catalysts. *J. Am. Chem. Soc.* **2008**, *130* (44), 14416−14417.

(2) (a) Hu, Q.; He, Z.; Peng, L.; Guo, C. Combining nickel and squaramide catalysis for the stereodivergent α-propargylation of oxindoles. *Nat. Synth.* **2022**, *1* (4), 322−331. (b) Wu, G.; Xu, H.; Liu, Z.; Liu, Y.; Yang, X.; Zhang, X.; Huang, Y. Asymmetric Organocatalysis Combined with Palladium Catalysis: Synergistic Effect on Enantioselective Mannich/α-Allylation Sequential Reactions of Pyrazolones in Constructing Vicinal Quaternary Stereocenters. *Org. Lett.* **2019**, *21* (19), 7708−7712.

(3) Ilina, K.; MacCuaig, W. M.; Laramie, M.; Jeouty, J. N.; McNally, L. R.; Henary, M. Squaraine Dyes: Molecular Design for Different Applications and Remaining Challenges. *Bioconj. Chem.* **2020**, *31* (2), 194−213.

(4) For selected examples, see: (a) Harmatys, K. M.; Cole, E. L.; Smith, B. D. In Vivo Imaging of Bone Using a Deep-Red Fluorescent Molecular Probe Bearing Multiple Iminodiacetate Groups. *Mol. Pharmaceutics* **2013**, *10* (11), 4263−4271. (b) Maeda, T.; Nguyen, T. V.; Kuwano, Y.; Chen, X.; Miyanaga, K.; Nakazumi, H.; Yagi, S.; Soman, S.; Ajayaghosh, A. Intramolecular Exciton-Coupled Squaraine Dyes for Dye-Sensitized Solar Cells. *J. Phys. Chem. C* **2018**, *122* (38), 21745−21754. (c) Arunkumar, E.; Ajayaghosh, A.; Daub, J. Selective Calcium Ion Sensing with a Bichromophoric Squaraine Foldamer. *J. Am. Chem. Soc.* **2005**, *127* (9), 3156−3164.

(5) Ajayaghosh, A. Chemistry of Squaraine-Derived Materials: Near-IR Dyes, Low Band Gap Systems, and Cation Sensors. *Acc. Chem. Res.* **2005**, *38* (6), 449−459.

(6) (a) Heng, L.; Ning, J.; Kong, F. Synthesis of Chiral Isosquaramides Containing Amino Acid. *Synth. Commun.* **2002**, *32* (20), 3093−3098. (b) Ohsedo, Y.; Miyamoto, M.; Tanaka, A.; Watanabe, H. Synthesis and electrochemical properties of symmetric squarylium dyes containing diarylamine. *Dyes Pigm.* **2014**, *101*, 261−269.

(7) For selected examples, see: (a) Davies, H. M. L.; Parr, B. T. Rhodium carbenes. In *Contemporary Carbene Chemistry*; Moss, R. A., Doyle, M. P., Eds.; Wiley: Hoboken, NJ, 2014; Chapter 12, pp 363−403. (b) Doyle, M. P.; Forbes, D. C. Recent advances in asymmtric catalytic metal carbene transformations. *Chem. Rev.* **1998**, *98*, 911. (c) Lindsay, V. N. G. Rhodium(II)-Catalyzed Cyclopropanation. In *Rhodium Catalysis in Organic Synthesis: Methods and Reactions*; Wileys-VCH: 2018; Chapter 15, pp 433−448. (d) Timmons, D. J.; Doyle, M. P. Chiral dirhodium(II) catalysts and their applications. In *Multiple Bonds Between Metal Atoms*; Cotton, F. A., Murillo, C. A., Walton, R. A., Eds.; Springer: Boston, MA, 2005; Chapter 13, pp 591−632.

(8) (a) Deng, Y.; Qiu, H. D.; Srinivas, H. P.; Doyle, M. Chiral Dirhodium(II) Catalysts for Selective Metal Carbene Reactions. *Curr. Org. Chem.* **2015**, *20* (1), 61−81. (b) Davies, H. M. L.; Manning, J. R. Catalytic C-H functionalization by metal carbenoid and nitrenoid insertion. *Nature* **2008**, *451* (7177), 417−424.

(9) (a) Davies, H. M. L.; Manning, J. R. C-H Activation as a Strategic Reaction: Enantioselective Synthesis of 4-Substituted Indoles. *J. Am. Chem. Soc.* **2006**, *128* (4), 1060−1061. (b) Davies, H. M. L.; Bruzinski, P. R.; Fall, M. J. Effect of diazoalkane structure on the stereoselectivity of rhodium(II) (S)-N-(arylsulfonyl) prolinate catalyzed cyclopropanations. *Tetrahedron Lett.* **1996**, *37* (24), 4133−4136.

(10) (a) Adly, G. F.; Maddalena, J.; Ghanem, A. Rh_2(*S*-1,2-NTTL)$_4$: A novel Rh_2(*S*-PTTL)$_4$ analog with lower ligand symmetry for asymmetric synthesis of chiral cyclopropylphosphonates. *Chirality* **2014**, *26* (11), 764−774. (b) Davies, H. M. L.; Briones, J. F. Rh_2(*S*-PTAD)$_4$-catalyzed asymmetric cyclopropenation of aryl alkynes. *Tetrahedron* **2011**, *67*, 4313−4317.

(11) (a) Xue, Y.-S.; Cai, Y.-P.; Chen, Z.-X. Mechanism and stereoselectivity of the Rh(ii)-catalyzed cyclopropanation of diazooxindole: a density functional theory study. *RSC Adv.* **2015**, *5* (71), 57781−57791. (b) DeAngelis, A.; Dmitrenko, O.; Yap, G. P. A.; Fox, J. M. Chiral Crown Conformation of Rh2(S-PTTL)4: Enantioselective Cyclopropanation with α-Alkyl-α-diazoesters. *J. Am. Chem. Soc.* **2009**, *131* (21), 7230−7231.

(12) (a) Rodriguez, K. X.; Pilato, T. C.; Ashfeld, B. L. An unusual stereoretentive 1,3-quaternary carbon shift resulting in an enantioselective RhII-catalyzed formal [4 + 1]-cycloaddition between diazo compounds and vinyl ketenes. *Chem. Sci.* **2018**, *9* (12), 3221−3226. (b) Rodriguez, K. X.; Kaltwasser, N.; Toni, T. A.; Ashfeld, B. L. Rearrangement of an Intermediate Cyclopropyl Ketene in a RhII-Catalyzed Formal [4 + 1]-Cycloaddition Employing Vinyl Ketenes as 1,4-Dipoles and Donor-Acceptor Metallocarbenes. *Org. Lett.* **2017**, *19* (10), 2482−2485. (c) Meloche, J. L.; Ashfeld, B. L. A Rhodium(II)-Catalyzed Formal [4 + 1]-Cycloaddition toward Spirooxindole Pyrrolone Construction Employing Vinyl Isocyanates as 1,4-Dipoles. *Angew. Chem., Int. Ed.* **2017**, *56* (23), 6604−6608. (d) Bonderoff, S. A.; Padwa, A. Polycyclic Ring Formation Using Bis-diazolactams for Cascade Stitching. *J. Org. Chem.* **2017**, *82* (1), 642−651. (e) Mercado-Marin, E. V.; Garcia-Reynaga, P.; Romminger, S.; Pimenta, E. F.; Romney, D. K.; Lodewyk, M. W.; Williams, D. E.; Andersen, R. J.; Miller, S. J.; Tantillo, D. J.; Berlinck, R. G. S.; Sarpong, R. Total synthesis and isolation of citrinalin and cyclopiamine congeners. *Nature* **2014**, *509* (7500), 318−324. (f) Huters, A. D.; Styduhar, E. D.; Garg, N. K. Total Syntheses of the Elusive Welwitindolinones with Bicyclo[4.3.1] Cores. *Angew. Chem., Int. Ed.* **2012**, *51* (16), 3758−3765.

(13) For an assessment of arene and *N*-substitution on diazo oxindole **6**, see Table S1 in the Supporting Information.
(14) Ghanem, A.; Gardiner, M. G.; Williamson, R. M.; Muller, P. First X-ray Structure of a *N*-Naphthaloyl-Tethered Chiral Dirhodium-(II) Complex: Structural Basis for Tether Substitution Improving Asymmetric Control in Olefin Cyclopropanation. *Chem.—Eur. J.* **2010**, *16*, 3291−3295.
(15) Hashimoto, S.-i.; Watanabe, N.; Sato, T.; Shiro, M.; Ikegami, S. Enhancement of enantioselectivity in intramolecular C-H insertion reactions of α-diazo β-keto esters catalyzed by chiral dirhodium(II) carboxylates. *Tetrahedron Lett.* **1993**, *34* (32), 5109−5112.
(16) Frisch, M. J.; Trucks, G. W.; Schlegel, H. B.; Scuseria, G. E.; Robb, M. A.; Cheeseman, J. R.; Scalmani, G.; Barone, V.; Petersson, G. A.; Nakatsuji, H.; Li, X.; Caricato, M.; Marenich, A. V.; Bloino, J.; Janesko, B. G.; Gomperts, R.; Mennucci, B.; Hratchian, H. P.; Ortiz, J. V.; Izmaylov, A. F.; Sonnenberg, J. L.; Williams-Young, D.; Ding, F.; Lipparini, F.; Egidi, F.; Goings, J.; Peng, B.; Petrone, A.; Henderson, T.; Ranasinghe, D.; Zakrzewski, V. G.; Gao, J.; Rega, N.; Zheng, G.; Liang, W.; Hada, M.; Ehara, M.; Toyota, K.; Fukuda, R.; Hasegawa, J.; Ishida, M.; Nakajima, T.; Honda, Y.; Kitao, O.; Nakai, H.; Vreven, T.; Throssell, K.; Montgomery, J. A., Jr.; Peralta, J. E.; Ogliaro, F.; Bearpark, M. J.; Heyd, J. J.; Brothers, E. N.; Kudin, K. N.; Staroverov, V. N.; Keith, T. A.; Kobayashi, R.; Normand, J.; Raghavachari, K.; Rendell, A. P.; Burant, J. C.; Iyengar, S. S.; Tomasi, J.; Cossi, M.; Millam, J. M.; Klene, M.; Adamo, C.; Cammi, R.; Ochterski, J. W.; Martin, R. L.; Morokuma, K.; Farkas, O.; Foresman, J. B.; Fox, D. J. *Gaussian 16, Revision C.01*; Gaussian, Inc.: Wallingford, CT, 2016.
(17) Azek, E.; Spitz, C.; Ernzerhof, M.; Lebel, H. A Mechanistic Study of the Stereochemical Outcomes of Rhodium-Catalysed Styrene Aziridinations. *Adv. Synth. Catal.* **2020**, *362* (2), 384−397.

https://doi.org/10.1021/acs.orglett.3c03344
Org. Lett. 2023, 25, 8156−8161